JACS
JOURNAL OF THE AMERICAN CHEMICAL SOCIETY

Article

pubs.acs.org/JACS

Photoinduced and Thermal Denitrogenation of Bulky Triazoline Crystals: Insights into Solid-to-Solid Transformation

Denisse de Loera, Antoine Stopin, and Miguel A. Garcia-Garibay*

Department of Chemistry and Biochemistry, University of California, Los Angeles, California 90095-1569, United States

Supporting Information

ABSTRACT: The photoinduced and thermal denitrogenation of crystalline triazolines with bulky substituents leads to the quantitative formation of aziridines in clean solid-to-solid reactions despite very large structural changes in the transition from reactant to product. Analysis of the reaction progress by powder X-ray diffraction, solid-state ^{13}C CPMAS NMR, solid-state FTIR spectroscopy, and thermal analysis has revealed that solid-to-solid reactions proceed either through metastable phases susceptible to amorphization or by mechanisms that involve a reconstructive phase transition that culminates in the formation of the stable phase of the product. While the key for a solid-to-solid transformation is that the reaction occurs below the eutectic temperature of the reactant and product two-component system, experimental evidence suggests that those reactions will undergo a reconstructive phase transition when they take place above the glass transition temperature.

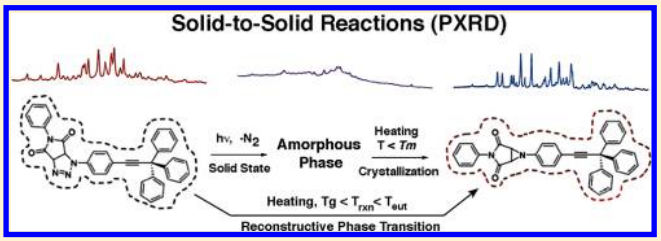

INTRODUCTION

Reports on reactions in organic crystals date back to 1834, when Trommsdorff described the yellowing and shattering that occurs when crystals of α-santonin are exposed to sunlight.[1−3] In fact, many reactions in crystals were documented through the 19th century.[4] An intuitive perspective based on size and shape confinement considerations, known as the *topochemical postulate*, was developed by Kohlshutter in the early 1920s[5] and put on a solid footing with structural data from single-crystal X-ray diffraction (XRD) in the 1960s by Schmidt and co-workers.[6,7] Until recently, the only guidelines to engineer reactions in crystals were based on the topochemical postulate, indicating that "reactions in crystals can only occur with a minimum of atomic and molecular motion". Accordingly, the feasibility of a given reaction in a crystalline solid depends on whether the geometric parameters that define the reactant(s) are preorganized[6] to form the product(s), and whether the reaction cavity[8] defined by the close-packing environment is preserved as a function of reaction progress. Topotactic control has been studied also in thermal[9] and photochemical[10] polymerization reactions which are governed by crystal packing. Although both thermal and photochemical reactions can occur under topochemical control, thermal activation requires excitation of normal vibrational modes and lattice phonons under thermal equilibrium, such that bond-breaking and bond-making events in the crystal must compete with melting. Conversely, photochemical activation generates localized excited states, which are not in thermal equilibrium with the rest of the lattice and are able to find reactive pathways before their excess energy is dissipated through the environment.[7]

Under these guidelines, the planning and execution of chemical reactivity in the solid state became a challenge in crystal engineering. However, it is impossible to design chemical reactions without acknowledging the importance of energetics. With that in mind, over the past few years we have suggested a general formulation of the topochemical postulate based on an energetic viewpoint: "Reactions in crystals may be accomplished with reactants that possess or transiently acquire large amounts of potential energy."[11,12] Structures that possess or acquire a high energy content may be capable of breaking and making bonds without having to experience rotations, collisions, and large-amplitude motions. At the same time, as suggested by the Hammond postulate, species with high potential energy tend to have early transition states and low activation barriers. Reactant-like transition states are ideal from a topochemical perspective because they require modest structural changes early on in their reaction coordinates.

We posit that there are a large number of reactants and reactions that meet these requirements.[8] In a recent test of this hypothesis, we began exploring the synthesis of ring-strained aziridines by the photoinduced denitrogenation of crystalline triazolines.[13] To our satisfaction, we confirmed that dry powdered crystals exposed to UV light with $\lambda \geq 290$ nm react without melting to give the expected aziridines **2** in excellent yields within 30−90 min. The reactions proceeded efficiently for several substituted triazolines (Scheme 1), suggesting that the transformation may be general and potentially useful for synthetic applications. It is known that the reaction proceeds through the formation of a 1,3-biradical by the extrusion of molecular nitrogen, and that the recombination of this intermediate generates the corresponding

Received: February 12, 2013
Published: April 2, 2013

   dx.doi.org/10.1021/ja401577p | J. Am. Chem. Soc. 2013, 135, 6626−6632

Scheme 1

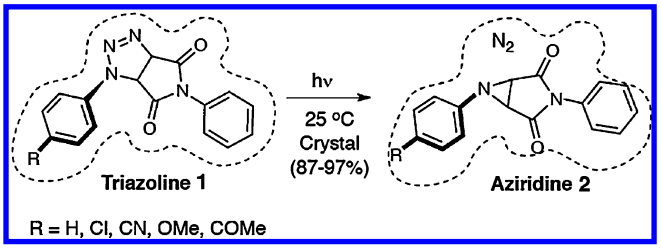

aziridine.[14] The release of gas molecules during reactions in crystal and its repercussion on the observed reactivity have been reported by McBride and co-workers with crystalline diacyl peroxides.[15] It was shown that molecules near a reaction site tend to rearrange to attenuate the local stress created by the formation of CO_2. It is reasonable to expect that similar stress will be observed upon release of N_2 in crystals of triazolines. While those structural changes are expected to affect the kinetics of elementary reactions as a function of conversion, they have no effect on the nature of the product formed in the case of the triazoline crystals.

Given the efficiency of the chemical transformations in Scheme 1, it was of interest to determine the nature of the physical changes accompanying the reaction: whether or not they are topochemical in nature. Based on our previous analysis of the phase changes that occur in solid-state reactions,[16] it is expected that all topochemical reactions must begin by formation of a solid solution of the product(s) in the lattice of the reactant. The most appealing and most demanding kind of transformations, commonly referred to as "topotactic" (or single crystal-to-single crystal),[16,17] occur in the same phase and retain single crystallinity as the reaction goes from starting material to the product [Figure 1, path (a)]. Other reactions are

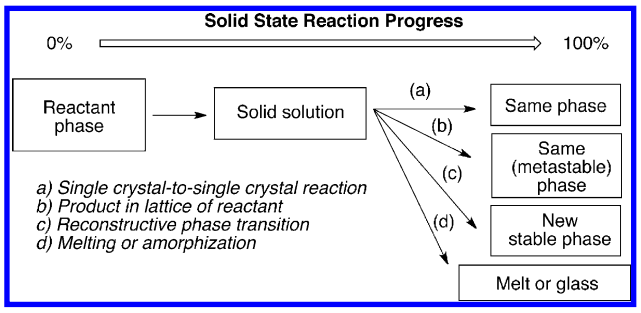

Figure 1. Potential phase changes accompanying solid-state reaction (for a detailed explanation please see main text).

able to continue in the crystal phase of the reactant, even if it is very different from the stable crystal phase of the final product [Figure 1, path (b)]. This was observed in our previous work, where powder X-ray diffraction (PXRD) after 100% conversion to aziridines **2** (Scheme 1) showed broadened peaks with a pattern that matched that of unreacted triazoline crystals.[13] These reactions have a tendency to lose long-range order and may not be suitable for single-crystal XRD analysis, but may be followed by PXRD. Another relatively common type of solid-to-solid reaction involves a reconstructive phase transition from the crystal of the reactant to the crystal of the product [Figure 1, path (c)].[18] Naumov and co-workers have reported this type of solid-state reaction in the thermochromism of dinitrobenzyl derivatives, finding that the phase transition is reversible.[19] In another example, Brillante and co-workers recently showed that the photoinduced solid-to-solid reaction of dinitroanthracene to anthraquinone occurs by a reconstructive process where molecular changes precede macroscopic changes in the crystal.[20] While the detailed mechanisms of these phase transitions and observed macroscopic changes are unknown, these reactions are only observed when the temperature of the reaction is below the eutectic point of the two-component phase diagram; otherwise, melting is observed. It is likely that these reactions proceed through small, steady-state amounts of amorphous phases, so that nucleation and growth of the product phase may only occur at temperatures above the corresponding glass transition temperature where molecular reorganization is permitted. There are reports on the nucleation and growth processes in the solid-state photoreaction of *α-trans*-cinnamic acid.[21] Finally, as indicated by Figure 1, path (d), there is an alternative where the starting crystal and subsequent mixed crystal phase are destroyed by melting or amorphization, depending on the reaction temperature in relation to the melting point and glass transition temperature of the product.

We recognized that the large changes in molecular size and shape that take place during the photoinduced denitrogenation of triazolines represent a challenge to the most widely accepted notions of topochemistry. With that in mind, we decided to investigate the solid-state reaction of triazolines containing very large bulky groups that could act as anchors, at either one or both ends of the molecule.

The compounds chosen to test the limits of topochemical restrictions in molecular crystals are illustrated in Scheme 2.

Scheme 2

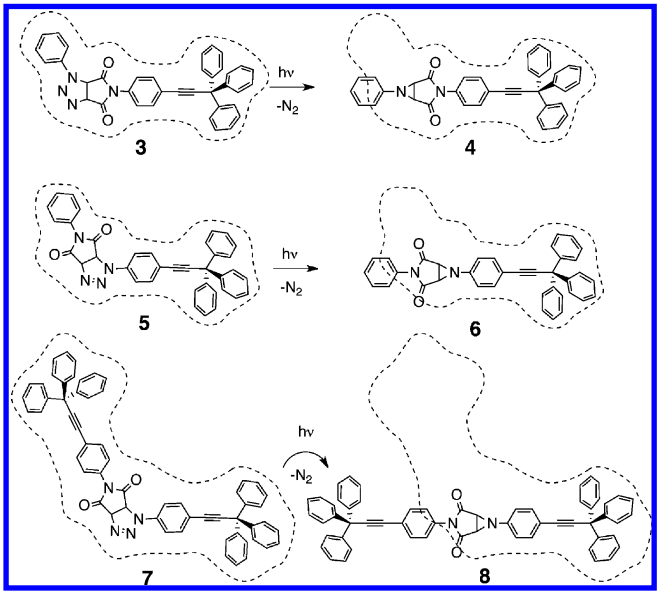

Compounds **3** and **5** are isomers that differ in the location of the bulky tritylacetylene, either on the phenyl group of the succinimide fragment or on the phenyl group of the triazoline. Compound **7** has bulky groups at each of the two positions (Scheme 2). A representation of the reaction cavity,[8] with the boundary formed by near neighbors in the crystal shown with a dotted line, in the structures in Scheme 2 highlights the fact that the size and shape of the reactant and the product are very different. The main question that arises when the structures of compounds **3**, **5**, and **7** are considered in the context of

dx.doi.org/10.1021/ja401577p | J. Am. Chem. Soc. 2013, 135, 6626−6632

topochemistry is whether their reactions may proceed, and what type of phase changes may occur as a result of such large structural changes. From the point of view of the structure of the chemically evolving system, it is of interest to find out whether the reacting solid may retain some of its original integrity as determined by its PXRD pattern. In this Article, we describe the synthesis of triazolines **3**, **5**, and **7** and confirm their efficient solid-state reactivity. We discovered that solid-to-solid photochemical reactions at ambient temperature proceed through metastable phases that eventually become amorphous, while a solid-to-solid thermal reaction carried out at 160 °C proceeds by a reconstructive phase transition mechanism. These and other observations suggested that amorphous phases are formed when there is a large mismatch between reactants and products, and that they can be trapped at low temperatures, presumably below the glass transition temperature. In contrast, analogous reactions occurring at higher temperatures take advantage of molecular motion that allows for the stable crystal phase of the product to nucleate and crystallize.

RESULTS AND DISCUSSION

Triazoline Synthesis and Characterization. Synthesis of compounds **3**, **5**, and **7** was carried out according to procedures reported in our previous work by dipolar cycloaddition of phenyl-substituted azides and maleimides (Scheme 3).[13]

Scheme 3

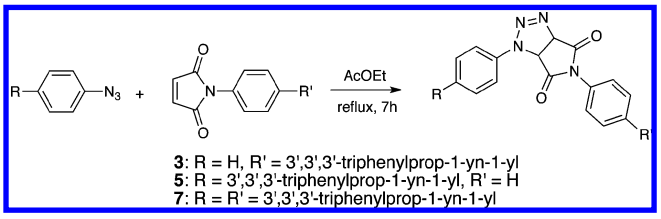

To prepare the starting materials bearing the bulky substituent, we synthesized 4-(3,3,3-triphenylpropyn-1-yl)-aniline **9** by Sonogashira coupling between 1,1,1-triphenyl-prop-2-yne and 4-bromoaniline (Scheme 4a). Phenylazides and *N*-phenylmaleimides were prepared according to published procedures[22,23] from aniline and compound **9**. Scheme 4b,c shows the synthesis of the azides **10** and **11** and maleimides **12** and **13**, respectively.

Triazolines **3**, **5**, and **7** were purified by column chromatography, and their molecular structures were characterized by FTIR, ^{1}H and ^{13}C NMR, and mass spectrometry. The main difference in the ^{1}H NMR spectra of the three triazolines is the displacement of the signal from the aromatic protons in the phenyl rings attached to the succinimide and triazoline moieties. Triazoline **3** presents the signals corresponding to the phenylene group linked to the succinimide moiety as an AA′BB′ system at ca. 7.33 and 7.60 ppm, and a set of signals at ca. 7.19, 7.42−7.45, and 7.71−7.72 ppm for the phenyl group that is attached to the triazoline. On the other hand, the triazoline **5** presents the corresponding succinimide *N*-phenyl signals at ca. 7.28, 7.43, and 7.48 ppm and the phenylene AA′BB′ pattern at ca. 7.56 and 7.67 ppm. Accordingly, triazoline **7** shows two AA′BB′ patterns, one at ca. 7.32 and 7.60 ppm that corresponds to the succinimide phenylene, and the other at ca. 7.56 and 7.66 ppm that corresponds to the phenylene group attached to the triazoline.

Aziridine Preparation and Characterization. Pure samples of aziridines **4**, **6**, and **8** were obtained in quantitative yields by heating polycrystalline samples of the corresponding triazolines for 30 min in an oil bath at 160 °C. Reactions of triazolines **3** and **7** yielded oily products that could be precipitated from dichloromethane. The thermal reaction of triazoline **5** carried out under these conditions occurred without melting in a relatively unusual solid-to-solid thermal reaction.

The identity of the aziridine products was confirmed by FTIR, ^{1}H and ^{13}C NMR, and mass spectrometry. The aziridine IR spectra showed the characteristic frequencies of the *N*-substituted aziridines,[24] which include ring stretching signals in the range of 1260−1280 cm^{-1}, ring CH wagging at 1170−1200 cm^{-1}, and ring CH twisting at 1320−1360 cm^{-1}, as well as the absence of the N═N stretching vibration at 1480−1490 cm^{-1} observed in the starting materials. The ^{1}H NMR spectra revealed the appearance of a broad singlet at ca. 3.87 ppm,

Scheme 4

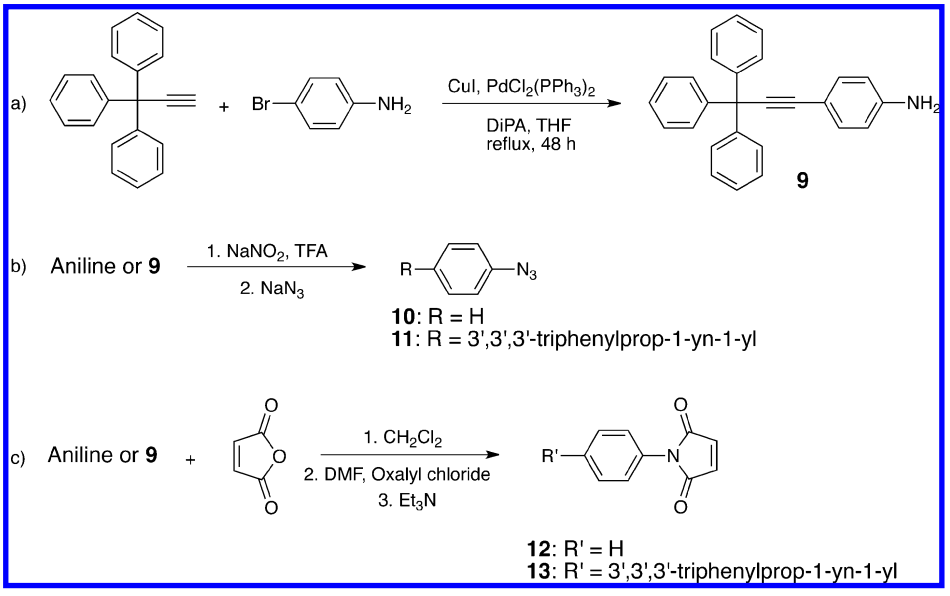

dx.doi.org/10.1021/ja401577p | J. Am. Chem. Soc. 2013, 135, 6626−6632

corresponding to the equivalent protons of the aziridine ring. The ^{13}C NMR spectra also showed only one signal corresponding to the equivalent bridgehead carbons in the aziridine at ca. 40 ppm.

Attempts to crystallize each of the three aziridines from different solvent mixtures yielded no crystals that were suitable for characterization by XRD, although analysis of a poorly diffracting twinned crystal of aziridine **8** grown from ethyl acetate led to a structural model that supports the expected connectivity (see Supporting Information). The molecular structure obtained in this manner is in agreement with a structure obtained by computational analysis of an aziridine analogue, *N*-(4-cyanophenyl)azirido-[2,3-*c*]-*N*-phenylmaleimide, with the B3LYP/6-31G* level of theory, which indicates that the *endo* configuration is ca. 1.0 kcal/mol more stable than the one where the *N*-phenylaziridine adopts the *exo* configuration.[25] The melting points of aziridines **4**, **6**, and **8** were 178−181, 260−262, and 142−148 °C, respectively.

Thermal Analyses and Thermal Denitrogenation. In order to investigate the thermal loss of nitrogen from triazolines **3**, **5**, and **7** in more detail, we carried out thermogravimetric analysis (TGA) and differential scanning calorimetry (DSC) measurements in the temperature range of 50−300 °C. The occurrence of the thermal reaction is readily identified by an exothermic peak in the DSC trace at a temperature that matches the loss of mass corresponding to the nitrogen molecule observed in the TGA. In the case of triazoline **3**, an endothermic transition at 138 °C was followed by a broad exothermic peak from 140 to 165 °C, indicating that melting occurs prior to the loss of nitrogen (Figure 2, top). For triazoline **5**, the DSC trace showed an exothermic peak at 159 °C corresponding to the loss of nitrogen followed by an endothermic peak at 258 °C, a temperature that is almost 100 °C higher (Figure 2, middle). It was subsequently shown that the second transition corresponds to the melting of aziridine **6**, thus confirming a solid-to-solid thermal reaction with a reconstructive phase transition mechanism, as indicated by path (c) in Figure 1. Finally, the DSC trace of triazoline **7** displayed only one broad exothermic peak at ca. 150−160 °C, which was matched by the loss of nitrogen in the TGA (not shown). As the melting point of the product is significantly lower (142−148 °C), the reaction proceeded in the liquid phase.

Photochemical Reactions and PXRD Analysis as Function of Reaction Progress. When dry powders of triazolines **3**, **5**, and **7** were exposed to UV light with $\lambda \geq 290$ nm from a medium-pressure 450-W Hg Hanovia lamp passed through a Pyrex filter at 298 K, smooth reactions yielded aziridines **4**, **6**, and **8** as the only products. The starting compound was always a microcrystalline powder, except for the compound **7**, which was an amorphous powder. Solid-to-solid transformations occurred with full conversion within 40−50 min under the conditions of the experiment described in the Supporting Information. Reaction progress was determined every 10 min by ^{1}H NMR by measuring the disappearance of the triazoline five-membered ring doublets at 4.98 and 5.90 ppm and the appearance of the aziridine singlets at 3.87 ppm. Several attempts to obtain suitable single crystals of either the starting materials or products for crystallography structure determination by X-ray had been unsuccessful. Therefore, to determine the nature of the photoinduced solid-to-solid reactions, we set out to measure the PXRD of the solid phases of starting triazolines **3**, **5**, and **7**, as well as those of the solvent-

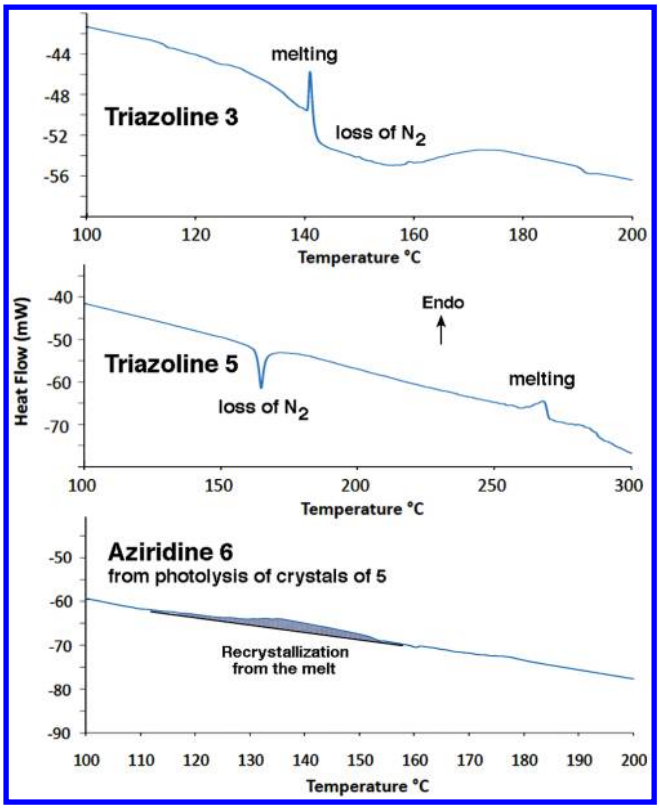

Figure 2. Differential scanning calorimetry traces of (top) triazoline **3** and (middle) **5**, illustrating melting and the loss of nitrogen. The bottom frame shows a thermogram of the amorphous phase of aziridine **6** obtained from photolysis of crystalline **5** at 298 K (melting not shown occurs at ca. 260 °C).

recrystallized aziridines **4**, **6**, and **8** in the range $2\theta = 5-50°$. While triazolines **3** and **5** presented characteristic sets of Bragg reflections typical of crystalline materials, samples of triazoline **7** showed no Bragg reflections, confirming that the corresponding solid is amorphous. By contrast, PXRD measurements of aziridines solids **4**, **6**, and **8** obtained by slow solvent evaporation revealed that all three samples are crystalline. With the stable end-points of the three reactions characterized, we carried out analogous measurements as a function of conversion, with samples taken from the photoreaction every 10 min. Optical microscopy was also used to monitor changes in the birefringence of a crystal of compound **5** as a function of reaction progress (see below). In order to determine whether the nitrogen gas generated during the reaction remains trapped in the crystals or escapes rapidly into the atmosphere, a small amount of microcrystalline **5** was irradiated in a capillary tube with a drop of mineral oil deposited with a syringe needle above the solid in order to trap a plug of air. An increase in the amount of gas as a function of increased irradiation time was detected as a displacement of the mineral oil, indicating that nitrogen escapes from the crystal during the time scale of the reaction. An estimate of the gas released during the experiment could be used to determine the extent of reaction, which was shown to be complete after ca. 40 min. We were able to confirm that all the nitrogen formed in the reaction had escaped from the crystals during the time of reaction with the help of TGA analyses of irradiated samples, which showed that there was no further loss of mass (N_2) when the sample was heated from ambient temperature to 115 °C. (For details of the experimental conditions and results, please see the Supporting

dx.doi.org/10.1021/ja401577p | J. Am. Chem. Soc. 2013, 135, 6626−6632

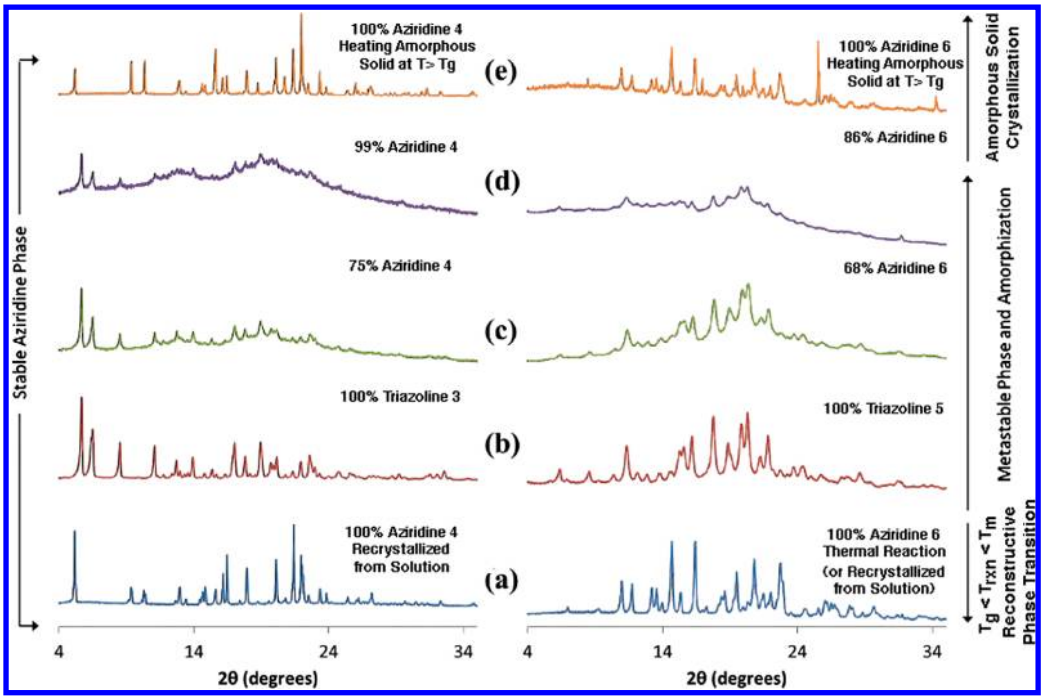

Figure 3. Comparison of the PXRD of triazolines **3** (left column) and **5** (right column) before reaction (b), and after different photochemical conversion values (c,d), with the amount of product indicated. Samples of aziridines **4** and **6** were obtained by crystallization of the amorphous phase by heating above T_g (e), by a solid-to-solid thermal reaction above the glass transition temperature and below melting in the case of **6** (a, right), or by recrystallization from solution of **4** (a, left). PXRD similar to that for **6** (a, right) was observed upon recrystallization from solution.

Information.) The evolution of gas may also be used to determine the conversion of the reaction by estimating the quantity of nitrogen released.

Starting with triazoline **5**, we discovered that the relatively sharp PXRD pattern of the starting material (Figure 3b, right) undergoes relatively minor changes at low conversion values (not shown), suggesting the formation of a solid solution that retains the packing arrangement of the starting material. When product accumulation reached values on the order of 60% (Figure 3c, right), the percentage of conversion was calculated on the basis of the NMR signals of the triazoline and aziridine bridgehead protons. Diffraction peaks broaden greatly until the pattern loses most of its signals when the reaction goes beyond ca. 85% (Figure 3d, right). Since none of the peaks of the stable aziridine are observed as the photochemical reaction proceeds at 298 K, one can safely conclude that there is not a reconstructive phase transition and that the photoreaction occurs by amorphization of the sample [Figure 1, path (d)]. ^{13}C CPMAS NMR showed a gradual increase in the signals line width, in agreement with the amorphization of the sample observed by PXRD (Supporting Information). Notably, when the amorphous photoproduct was heated neat to 160 °C, well below the melting point of aziridine **6** (260−262 °C), we were able to obtain a PXRD pattern essentially identical to that of the solvent-recrystallized aziridine (Figure 3e, right). Furthermore, the same powder pattern was obtained when crystals of triazoline **5** were heated to 160 °C (Figure 3a, right), indicating a clean solid-to-solid reaction by a reconstructive phase transition mechanism.[26] Taken together, these observations suggest that the difference between the low-temperature amorphization and the high-temperature reconstructive phase transition should be related to the rigidity of the sample, suggesting that crystallization from amorphous phases is likely to occur above the corresponding glass transition temperature at $T \approx 110$ °C (Figure 2, bottom). Notably, DSC analysis of amorphous aziridine samples obtained by solid-state photoreaction of triazoline **5** does not show a clear glass transition but rather a very broad endothermic signal between ca. 110 and 160 °C (Figure 2, bottom) that is consistent with crystallization of the amorphous material into the polycrystalline aziridine phase.

The photodenitrogenation of compound **5** was also studied by optical microscopy with a small crystal exposed to UV light for eight periods of 5 min (Figure 4). While no macroscopic changes were observed and the crystal appeared intact when viewed under reflected white light (Figure 4, left column), a

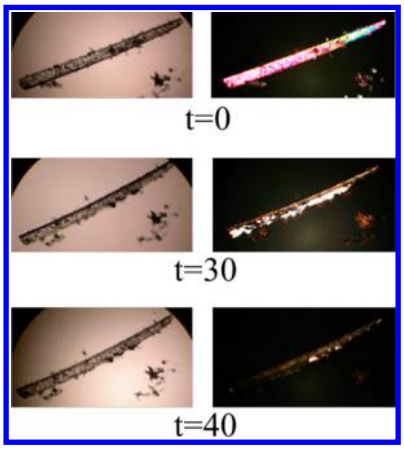

Figure 4. Optical microscopy pictures of a crystal of triazoline **5** before and after irradiation (time indicated in minutes). Images obtained with cross polarizers (right column) illustrate the loss of crystallinity by the loss of birefringence. Images obtained with normal illumination (left column) show no apparent changes.

dx.doi.org/10.1021/ja401577p | J. Am. Chem. Soc. 2013, 135, 6626−6632

progressive loss of birefringence was observed as a function of increased exposure (Figure 4, right column). The crystal lost most of its birefringence after 40 min, and it was later confirmed that full conversion to aziridine **6** had taken place. This experiment clearly revealed that the solid becomes amorphous with increased conversion values, suggesting a process that occurs along path (d) in Figure 1. By comparison, the formation of anthraquinone from dinitroanthracene recently reported by Brillante and co-workers proceeds along path (c) in Figure 1,[20] with the crystal showing notable changes of shape without amorphization. Even though reaction progress modifies the crystal (amorphization or restructuration) in these and other cases, the reaction still occurs in the solid state.

The results obtained upon photolysis and PXRD analysis of triazoline **3** at 298 K were analogous to those described above (Figure 3, left). The powder pattern remained relatively unchanged up to ca. 75% conversion, when it started broadening in a significant manner. Irradiation to full conversion transformed the sample into a largely amorphous solid with a PXRD that has only small residual signals, suggesting a very small degree of crystallinity or a very small fraction of a crystalline phase. The fully converted solid was shown to have a glass transition process at 130 °C, and after softening the sample crystallized into the stable crystalline phase of aziridine **4**. The reaction of triazoline **7** to aziridine **8** was not investigated in as much detail, considering that the sample starts as an amorphous solid and the end point of the photoreaction at ambient temperature is also an amorphous solid.

On the basis of these results, we propose a qualitative phase diagram as a function of reaction progress that accounts for the reaction modes indicated in Figure 1. Shown in Figure 5, the

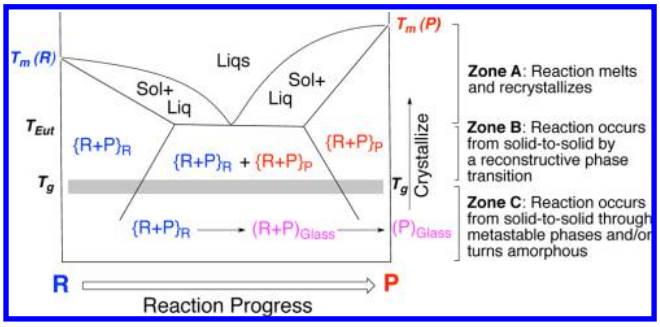

Figure 5. Schematic phase diagram of the triazoline denitrogenation reaction progress (for a detailed explanation please see main text).

phase diagram has three temperature zones that are expected to display different phase behavior when crystalline R is the starting material. Reactions occurring in the higher temperature zone, indicated with label A, will start in the solid state in a reactant-like phase $\{R+P\}_R$ until its composition reaches the solid−liquid line and the reaction begins to melt. If the melting point of P is higher than that of R, as illustrated in the figure, the product mixture may recrystallize in a product-like phase $\{R+P\}_P$ when its composition reaches the values of the solid−liquid line near the product. If the melting point of R is much higher than that of P and the reaction occurs at a temperature that is above the melting point of the product, the reaction would be completed in a liquid phase. Reactions carried out at temperatures between the eutectic point and the glass transition temperatures of the two-component system are labeled as occurring in zone B. These reactions are expected to start in the crystalline phase of the reactant $\{R\}_R$, proceed through the reactant-like mixed crystalline phase $\{R+P\}_R$ until the solubility limit of the product is reached, and then transform into a metastable reactant-like phase, or become amorphous, until the composition of the product-like crystal $\{R+P\}_P$ is reached and the sample can recrystallize into the new product phase $\{P\}_P$. In our experience, these reactions are common and can be documented as occurring by a reconstructive phase transition mechanism. Finally, we propose that reactions taking place at temperatures that are well below the glass transition temperature of the two-component system (zone C) do not allow molecules to undergo the motions required for nucleation and crystallization and therefore must proceed in a metastable reactant-like phase or, when the structural changes on going from reactant to product are too drastic, become amorphous. We propose that the solid-state photochemical reactions of triazolines **3** and **5** take place in zone C, as seen through the loss of birefringence of the solid (Figure 4), with reactions proceeding along metastable and amorphous phases that can be recrystallized by heating the solid product above the glass transition temperature. By contrast, we deduce that the thermolysis of triazoline **5** occurs above the glass transition temperature (T_g), and well below the eutectic temperature (T_{eut}) so that liquid phases are not encountered, as shown by calorimetric analysis (Supporting Information). Under these conditions, the thermal reaction proceeds by a solid-to-solid reconstructive phase transition mechanism along zone B. On the other hand, calorimetric analysis of crystalline triazoline **3** shows that it melts and then rapidly loses nitrogen, such that the product is formed in the liquid phase along zone A. Finally, triazoline **7** starts reacting in an amorphous phase, and the thermal reaction occurs when the sample softens. As suggested in Figure 5, it seems reasonable that the types of phases involved in these reactions, whether crystalline, amorphous, or liquid, will depend on the physical properties of the reactant, product, and eutectic mixtures, as well as on their ability to form mixed crystalline phases.

■ CONCLUSIONS

Using the photoinduced denitrogenation of crystalline triazolines with bulky substituents as a test model to challenge the topochemical postulate, we were able to document several types of solid-to-solid reactions that follow different phase transformation mechanisms. Despite very large differences in size and shape between the triazoline reactants and the aziridine products, photoinduced solid-to-solid reactions proceeded to completion within 50 min to yield the corresponding aziridines in amorphous phases and ca. 100% yields. By contrast, depending on the substituents, the thermal reactions were shown to occur upon melting, after softening, or by a solid-to-solid reaction that occurs by a reconstructive phase transition mechanism. It was also shown that amorphous phases obtained by photochemical irradiation could be recrystallized by heating, presumably above the glass transition temperature. The results obtained in this study increase our understanding of phase transformation mechanisms involved in solid-to-solid reactions and thus may help in the development of novel green chemistry strategies and materials science applications.

■ ASSOCIATED CONTENT

Supporting Information

Synthesis and characterization of all compounds; ^{1}H and ^{13}C NMR and mass spectra; DSC, PXRD, ^{13}C CPMAS, NQS, and

dx.doi.org/10.1021/ja401577p | J. Am. Chem. Soc. 2013, 135, 6626−6632

solid-state FTIR studies. This material is available free of charge via the Internet at http://pubs.acs.org.

AUTHOR INFORMATION

Corresponding Author

mgg@chem.ucla.edu

Notes

The authors declare no competing financial interest.

ACKNOWLEDGMENTS

This research was supported by NSF grants DMR1101934 and CHE-0844455. We thank UC-Mexus for a postdoctoral fellowship to D.d.L. We also thank B. Rodriguez-Molina for ^{13}C CPMAS NMR measurements.

REFERENCES

(1) Trommsdorff, S. *Ann. Chem. Pharm.* **1834**, 11.

(2) Matsuura, T.; Sata, Y.; Katsuyuki, O. *Tetrahedron Lett.* **1968**, *44*, 4627.

(3) Natarajan, A.; Tsai, C. K.; Khan, S. I.; McCarren, P.; Houk, K. N.; Garcia-Garibay, M. A. *J. Am. Chem. Soc.* **2007**, *129*, 9846.

(4) Ramamurthy, V.; Venkatesan, K. *Chem. Rev.* **1987**, *87*, 433.

(5) (a) Kohlshutter, V. *Anorg. Allg. Chem.* **1918**, *105*, 121. (b) Kohlshutter, V. *Kolloid-.* **1927**, *42*, 254. (c) Kohlshutter, V. *Z. Anorg. Allg. Chem.* **1920**, *111*, 193.

(6) (a) Cohen, M. D.; Schmidt, G. M. J. *J. Chem. Soc.* **1964**, 1996. (b) Cohen, M. D.; Schmidt, G. M. J.; Sonntag, F. I. *J. Chem. Soc.* **1964**, 2000. (c) Schmidt, G. M. J. *J. Chem. Soc.* **1964**, 2014.

(7) Examples of topochemical control reactions: (a) Ramamurthy, V.; Venkatesan, K. *Chem. Rev.* **1987**, *87*, 433. (b) MacGilvray, L.; Papaefstathiou, G. S. Solid-state reactivity/topochemistry. In *Encyclopedia of supramolecular chemistry*; Atwood, J. L., Steed, J. W., Eds;, Taylor & Francis: New York, 2004; pp 1316−1321. (c) Mandel, S. M.; Singh, P. N. D.; Muthukrishnan, S.; Chang, M.; Krause, J. A.; Gudmundsdottir, A. D. *Org. Lett.* **2006**, *8*, 4207. (d) Sankaranarayanan, J.; Bort, L. N.; Mandel, S. M.; Chen, P.; Krause, J. A.; Brooks, E. E.; Tsang, P.; Gudmundsdottir, A. D. *Org. Lett.* **2008**, *10*, 937.

(8) Cohen, M. D. *Angew. Chem., Int. Ed.* **1975**, *14*, 386.

(9) Xu, Y.; Smith, M. D.; Geer, M. F.; Pellechia, P. J.; Brown, J. C.; Wibowo, A. C.; Shimizu, L. S. *J. Am. Chem. Soc.* **2010**, *132*, 5334.

(10) (a) Gnanaguru, K.; Ramasubbu, N.; Venkatesan, K.; Ramamurthy, V. *J. Org. Chem.* **1985**, *50*, 2337. (b) Nomura, S.; Itoh, T.; Nakasho, H.; Uno, T.; Kubo, M.; Sada, K.; Inoue, K.; Miyata, M. *J. Am. Chem. Soc.* **2004**, *126*, 2035.

(11) (a) Garcia-Garibay, M. A. *Acc. Chem. Res.* **2003**, *36*, 491. (b) Garcia-Garibay, M. A.; Shin, S.; Sanrame, C. *Tetrahedron* **2000**, *56*, 6729. (c) Campos, L. M.; Garcia-Garibay, M. A. In *Reactive Intermediates*; Platz, M. S., Jones, M., Moss, R., Eds.; Wiley: Hoboken, NJ, 2007.

(12) Alternative mechanisms could involve reactions that occur by quantum mechanical tunneling from molecules that are structurally predisposed to react from their lower vibrational states: (a) Johnson, B. A.; Garcia-Garibay, M. A. *The Spectrum* **1998**, *11*, 1. (b) Garcia-Garibay, M. A.; Gamarnik, A.; Bise, R.; Pang, L.; Jenks, W. S. *J. Am. Chem. Soc.* **1995**, *117*, 10264.

(13) de Loera, D.; Garcia-Garibay, M. A. *Org. Lett.* **2012**, *14*, 3874.

(14) (a) Sheiner, P. *J. Am. Chem. Soc.* **1968**, *90*, 988. (b) Meier, H.; Zeller, K. P. *Angew. Chem., Int. Ed. Engl.* **1977**, *16*, 835. (c) Schultz, A. G.; Sha, C.-K. *J. Org. Chem.* **1980**, *45*, 2040. (d) Tukada, H. *Chem. Commun.* **2000**, 63. (e) Chen, Y.-J.; Hung, H.-C.; Sha, C.-K.; Chung, W.-S. *Tetrahedron* **2010**, *66*, 176.

(15) (a) McBride, J. M. *Acc. Chem. Res.* **1983**, *16*, 304. (b) McBride, J. M.; Segmuller, B. E.; Hollingsworth, M. D.; Mills, D. E.; Weber, B. A. *Science* **1986**, *234*, 830.

(16) Keating, A. E.; Garcia-Garibay, M. A. Photochemical Solid-To-Solid Reactions. In *Organic and Inorganic Photochemistry*; Ramamurthy, V., Schanze, K., Eds.; Marcel Dekker: New York, 1998; Vol. *2*, pp 195−248.

(17) (a) Friscic, T.; MacGillivray, L. R. *Z. Kristallogr.* **2005**, *220*, 351. (b) Barbour, L. J. *Aust. J. Chem.* **2006**, *59*, 595. (c) Halasz, I. *Cryst. Growth Des.* **2010**, *10*, 2817. (d) Nieuwendaal, R. C.; Mattler, S. J.; Bertmer, M.; Hayes, S. E. *J. Phys. Chem. B* **2011**, *115*, 5785.

(18) Choi, T.; Cizmeciyan, D.; Kahn, S. I.; Garcia-Garibay, M. A. *J. Am. Chem. Soc.* **1995**, *117*, 12893.

(19) (a) Naumov, P.; Sakurai, K. *Cryst. Growth Des.* **2005**, *5*, 1699. (b) Lee, J. H.; Naumov, P.; Chung, I. H.; Lee, S. C. *J. Phys. Chem. A* **2011**, *115*, 10087.

(20) Salzillo, T.; Bilotti, I.; Della Valle, R. G.; Venuti, E.; Brillante, A. *J. Am. Chem. Soc.* **2012**, *134*, 17671.

(21) (a) Bertmer, M.; Nieuwendaal, R. C.; Barnes, A. B.; Hayes, S. E. *J. Phys. Chem. B* **2006**, *110*, 6270. (b) Nieuwendaal, R. C.; Bertmer, M.; Hayes, S. E. *J. Phys. Chem. B* **2008**, *112*, 12920.

(22) Braish, T. F.; Fox, D. E. *Synlett* **1992**, *12*, 979.

(23) Leyva, E.; de Loera, D.; Jiménez-Cataño, R. *Tetrahedron Lett.* **2010**, *51*, 3978.

(24) Spell, H. L. *Anal. Chem.* **1967**, *39*, 185.

(25) Computational analysis using B3LYP/6-31G* for *N*-(4-cyanophenyl)azirido-[2,3-*c*]-*N*-phenylmaleimide: *exo* configuration, −969.0976 hartree; *endo* configuration, −969.0993 hartree; difference, 1.038 kcal/mol.

(26) Similar observations were documented by solid-state ^{13}C CPMAS NMR and solid-state FTIR analysis. Please see the Supporting Information.